

Stopping Power in Insulators and Metals without Charge Exchange

S. P. Møller,¹ A. Csete,² T. Ichioka,² H. Knudsen,² U. I. Uggerhøj,² and H. H. Andersen³

¹*Institute for Storage Ring Facilities, University of Aarhus, DK-8000 Aarhus C, Denmark*

²*Department of Physics and Astronomy, University of Aarhus, DK-8000 Aarhus C, Denmark*

³*Ørsted Laboratory, Niels Bohr Institute, Universitetsparken 5, DK-2100 København Ø, Denmark*

(Received 18 November 2003; published 21 July 2004)

The slowing-down process of pointlike charged particles in matter has been investigated by measuring the stopping power for antiprotons in materials of qualitatively very different nature. Whereas the velocity-proportional stopping power observed for metal-like targets such as aluminum over a wide energy range of 1–50 keV is in agreement with expectations, it is surprising that the same velocity dependence is seen for a large band-gap insulator such as LiF. The validity of these observations is supported by several measurements with protons and several checks of the target properties. The observations call for both a qualitative explanation and a quantitative theoretical model.

DOI: 10.1103/PhysRevLett.93.042502

PACS numbers: 29.30.Aj, 34.50.Bw, 61.85.+p

Ever since the discovery of the constituents of atoms in the beginning of the 20th century, the interaction of charged particles with matter has been of topical interest [1]. This interest has partly been of a fundamental nature to learn about the particles and their interaction. In addition, the interest has been spurred by practical aspects relating to the penetration of charged particles through materials. When a proton or antiproton (\bar{p}) traverses matter, it will lose energy mainly in so-called electronic collisions with the target atoms, whereby the atoms are excited or ionized. Only at very low projectile energies is there a significant energy loss from nuclear collisions, where the target atoms recoil as a whole.

Solid targets are only approximately described in the stopping process as assemblies of free atoms. In particular, the atoms in the material overlap and rearrangements of the outer electrons take place. One prime example here is phase effects, resulting in differences in the stopping of, e.g., a solid metal and its vapor. Furthermore, the so-called Bragg rule, which predicts the stopping cross section of a compound as the sum of the stopping cross sections of the constituents, is only approximate.

The slowing down is mainly characterized by the stopping power $-dE/dx$. At low energies it is often assumed that the stopping power is proportional to the projectile velocity. This is partly based on experimental evidence, and partly on the free-electron-gas approximation [2,3], which at low projectile energies results in a velocity-proportional stopping power. The success of this approximation is comprehensible for metals, where the outer electrons form an almost free electron gas. We have recently confirmed this approximation with antiproton measurements [4]. Antiprotons are particularly well suited to test the fundamental stopping mechanisms since charge exchange processes, which are very important for positive particles, are absent, and the projectile charge is always -1 . Particles of a negative charge are subject to a lower stopping power than positive particles due to the polarization of the target electrons. This so-called Barkas

effect, which was first observed as a range difference between positive and negative pions [5], has in the last decade been studied in detail with antiprotons [4,6].

Departures from a velocity-proportional stopping have been searched for a long time as a way of exploring the region of validity of the free-electron gas approximation. So far, for positive particles deviations from velocity-linear stopping at low energies have been observed only in the case of gas-phase He [7] and Ne [8] targets. They were interpreted as being due to a so-called threshold effect, which appears when the projectile is too slow to excite the target electrons. Semrad [9] suggested that this effect should be discernible as a departure from velocity proportionality below a projectile energy of around $500E_g$, where E_g is the minimum excitation energy of the target. Already Fermi and Teller [2] found for the case of insulators that the condition $mv_m v > E_g$ is necessary to treat the slowing-down process as in a metal, i.e., to get $-dE/dx \propto v$. Here m , v_m , and v denote the electron mass, the velocity of the “active” electrons in the insulator, and the velocity of the penetrating particle, respectively. This condition agrees with Semrad’s expression. For LiF where $E_g \simeq 14$ eV we find $E > 7$ keV.

Threshold effects were observed in the energy loss of protons due to inner-shell electrons [10], but these effects are small as it is the loosely bound electrons which give the dominating contribution to the stopping. In surface scattering of protons on LiF targets a large threshold effect has been observed [11]. Measurements utilizing negative muons have addressed the question of velocity proportionality in MgF_2 and kapton insulators [12,13] and claim to find a reduced energy loss below 44 and 2.2 keV/amu, respectively, which were ascribed to an effect of the band gap. These measurements, however, were indirect and in some cases suffered from limited statistical accuracy.

It was therefore a surprise when velocity proportionality was observed for the stopping power for protons of energies substantially lower than $500E_g$ for insulators

such as LiF, Al₂O₃, and SiO₂ [14]. This was tentatively explained as being due to a sizable contribution to the stopping from electron promotion processes, where electrons are promoted to molecularlike orbitals [11,15,16]. In the band-structure description of solids, the large band gap is therefore locally reduced by the presence of the positive projectile.

A very successful recent theory for calculating stopping powers is the so-called binary model by Sigmund and Schinner [17]. This nonperturbative classical theory includes Bohr's classical result for the distant collisions and Rutherford's law for close collisions. In addition to being able to predict accurately stopping powers for ions [18], it produces velocity-proportional stopping in LiF without recourse to electron promotion effects [19–21]. Similarly, measurements in Al₂O₃ and SiO₂ can be reproduced by a dielectric formalism down to energies of 2 keV [22]. These procedures, however, neglect the contribution from capture and loss processes, a channel known to have a dominating contribution to the energy loss.

The motivation for the present study is to look for deviations from velocity-proportional stopping, but with antiprotons, where charge-exchange and electron promotion effects are excluded. The experimental procedures follow closely those described in [23]. The uncertainty in these first measurements was dominated by the large variations in the number of particles from pulse to pulse. A major improvement has been accomplished at the facility since then, and hence much more accurate measurements, over a wider energy range, are presented here.

In short, the antiproton decelerator (AD) at CERN delivers around 10^7 antiprotons in a pulse of 200 nsec duration at a kinetic energy of 5.3 MeV with a repetition time of about 2 min. A radio frequency quadrupole subsequently decelerates this beam to an energy that can be varied between 0 and 120 keV.

The experimental apparatus, see Fig. 1, used in the determination of the stopping powers, is based on two 90° electrostatic spherical analyzers (ESA). The first analyzer is used to select an incident beam with a small energy spread around the energy E_1 . After traversal of the target foil of thickness Δx , a second analyzer measures the exit energy of the beam E_2 . The stopping power is then determined as $-dE/dx = (E_1 - E_2)/\Delta x$ at the average energy $(E_1 + E_2)/2$. The \bar{p} beam is detected by two-stage channel-plate detectors with optical readout by charge coupled device cameras from a phosphor screen. One detector is positioned after the first analyzer, for tuning of the incident beam, and another one after the second analyzer; see Fig. 1. The whole setup has been thoroughly calibrated and tested using protons of known energy [4,23].

The metal foils used in the experiment are mounted on nickel meshes with 88% transmission. The LiF targets are evaporated on a 200 Å carbon backing foil, which is mounted on the same type of nickel meshes. Half of the carbon backing is blocked during the evaporation process.

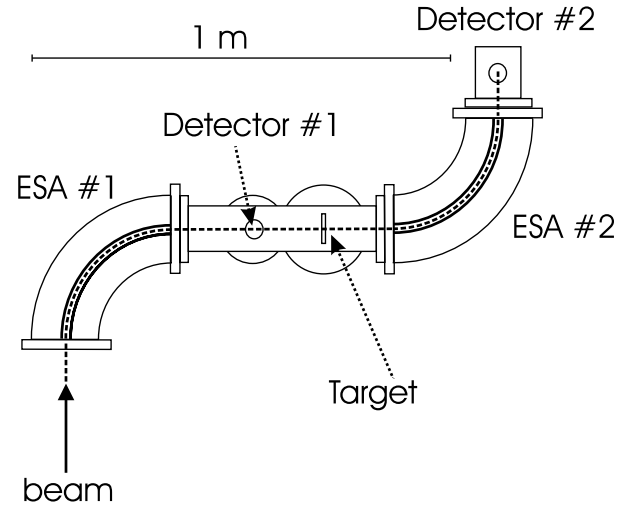


FIG. 1. Schematic diagram of the stopping power experiment. The target foil is insulated and can be raised to a bias voltage in order to vary the projectile impact energy.

In this way, the energy loss can be measured simultaneously for particles traversing the carbon foils and particles traversing carbon and LiF to allow direct subtraction of the carbon energy loss. An example of a scan of the voltage of the second analyzer is shown in Fig. 2 for a typical \bar{p} beam. The two energy-loss peaks from C and C + LiF are seen. The stopping power measurements of LiF for antiprotons are shown in Fig. 3 with filled circles and triangles. Reference proton measurements were made using a small proton accelerator, and these are shown as open triangles. We observe consistency between measurements on different foils. The proton and antiproton measurements are partly made on the same foils, partly on foils evaporated simultaneously. The dotted line is the “recommended” [24] stopping power for protons. The

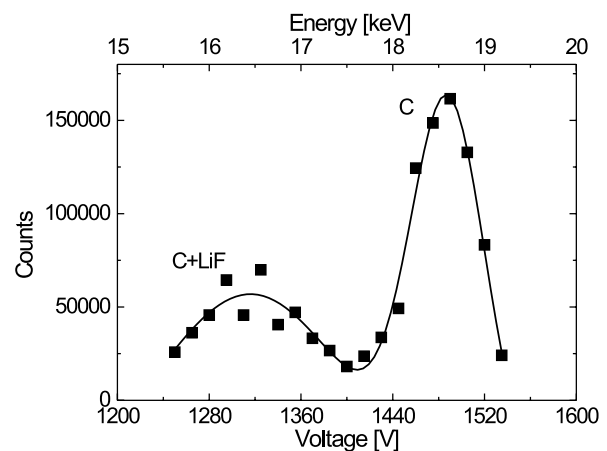


FIG. 2. Voltage scan of the second deflector showing the energy-loss peaks from C and C + LiF and the curve shows a fit of the data with two Gaussians. The collision energy is 33 keV due to a bias applied to the foil. The scatter of the points is mainly due to pulse-to-pulse variations of the AD.

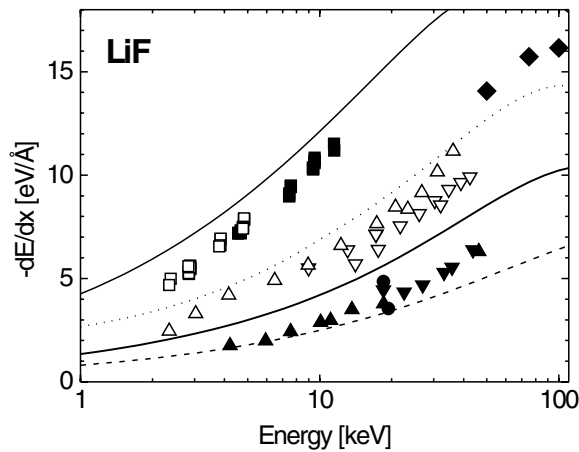


FIG. 3. Measured antiproton (▲, ▼, both 400 Å foils; ● 200 Å) and proton (△ 200 Å; ▽ 400 Å) stopping powers of LiF. The squares are the proton and deuteron measurements from [14] and ◆ are from [25]. See the text for an explanation of the curves.

first calculations by Sigmund's group are shown as the dashed line for antiprotons [19,20]. Their more recent calculations [21] for protons (upper line) and antiprotons (lower full line) are also shown.

The thickness of the foils is an important issue. First of all the thicknesses were measured using a quartz balance giving the thicknesses mentioned in Fig. 3. In addition we have performed thickness measurements using Rutherford backscattering (RBS) with 350 keV protons. The thicknesses were determined relative to reference gold foils. The thickness of these Au foils has in turn been determined by weighing and by RBS with 4 MeV alpha particles. These last two measurements are absolute thickness determinations. From these measurements we infer that the foils found to be ≈ 400 Å from the evaporation process have a thickness of (375 ± 20) Å, in good agreement. A more accurate determination cannot be made due to background and due to the deviations from Rutherford scattering of the fluorine scattering cross section.

We have made transmission electron microscopy on the foils. The foils are rather homogenous, but we do see grain structures with grain sizes of a few hundred Å, i.e., of approximately the same size as the foil thicknesses.

Our proton measurements are around 15% lower than the values recommended by ICRU [24], but the same velocity dependence is seen. In addition, they seem to meet the data from [25] at high energy. However, our measurements are at variance with other existing data, namely, the relatively recent measurements from Eder *et al.* [14], which are also shown on the figure as open and filled squares. The reason for this discrepancy is not understood and requires further investigations. The LiF \bar{p} stopping powers are lower than those of protons by around 50% over the energy range covered, 2–50 keV, due to the Barkas effect. In addition we observe a velocity dependence, which appears to be linear. To investigate

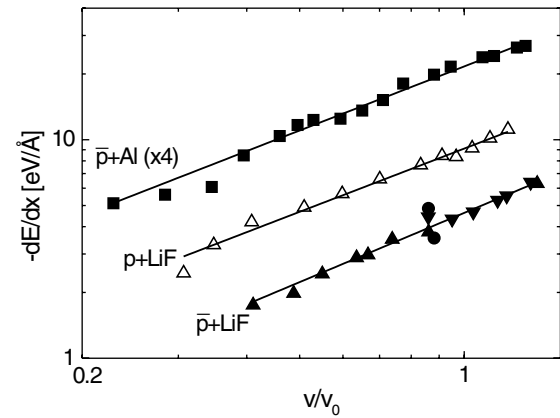


FIG. 4. Measured stopping powers for antiprotons in LiF (▲, ▼, ●) and Al (■) and for protons in LiF (△) as a function of velocity relative to the Bohr velocity. The lines represent fits to the data.

this in detail, the stopping power measurements as function of velocity are shown on a doubly logarithmic plot in Fig. 4. The data were fitted to the function av^b , where a and b are free parameters. The emerging exponents b obtained for protons and antiprotons on LiF are 0.96 ± 0.04 and 1.05 ± 0.07 , respectively, indeed very close to velocity proportionality.

To support the measurements on LiF and for comparison, we also present new accurate measurements of aluminum stopping powers for antiprotons, obtained with the same apparatus, in Figs. 4 and 5 as filled squares. As expected a velocity-proportional stopping power is seen with an exponent $b = 0.97 \pm 0.03$. The open symbols are our measured proton stopping powers. In Fig. 5 the diamonds are \bar{p} measurements from [6]. The curves denote the recommended stopping power for protons [24] (dotted line), Sigmund and Schinner's theory for antiprotons [17] (dashed line), and Sørensen's electron-gas calculation [26] (full line). The agreement with theory (for \bar{p}) and with ICRU (for p) supports our experimental method.

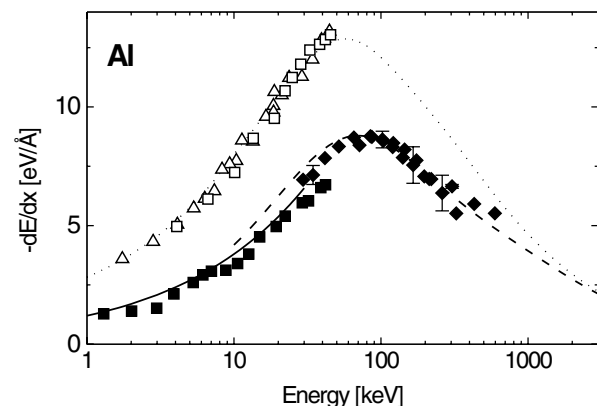


FIG. 5. Measured antiproton (■) and proton (△, □) stopping powers of Al (this work). The data ◆ are from [6]. See the text for an explanation of the curves.

The antiproton stopping power of LiF is observed to be very near velocity proportional. This is surprising and requires an explanation. Starting with the first observation of a much steeper than linear velocity dependence of the proton stopping power in helium below 10 keV [7], this could be readily accounted for by calculations [8,9,27]. The explanation was a threshold effect due to the rather large minimum energy transfer ($E_g = 19.8$ eV) of protons in helium. Coulomb trajectory effects were estimated to be negligible. A similar effect was seen in neon [8], where the minimum excitation energy E_g is 16.7 eV. Hence it was surprising that wide-band-gap insulators such as Al_2O_3 , SiO_2 , and LiF ($E_g = 8, 8,$ and 14 eV, respectively) showed no influence of the band gap on the velocity dependence of the proton stopping power [14]. Qualitatively, this was explained as a local reduction of the band gap with respect to the undisturbed crystal due to the perturbing positive projectile. Electrons are promoted from bound states in LiF to unoccupied states via formation of molecular orbitals, the incoming proton being one of the atomic centers.

The nonappearing threshold effect and linear velocity dependence for antiprotons cannot be explained by such a promotion mechanism due to the repulsion between the \bar{p} and the target electrons. Of course the presence of a slow, negative projectile may also disturb the crystal electronic states locally, but it is hard to see why this disturbance, if at all of importance, should have precisely the same effect on negative projectile stopping powers as has the suggested promotion effect for positive projectiles. Hence we need at least one new mechanism, not based on promotion, to explain the antiproton data. In addition, this mechanism might also challenge the electron promotion model for positive particles.

We point out that a significantly steeper velocity dependence than proportionality has been observed only for gas targets. This might indicate a connection to the phase of the target.

Finally we also mention the measurements of energy losses of protons scattered on LiF surfaces [11]. Here a velocity-proportional stopping power is also observed, but in addition a threshold at around 1 keV is seen. Furthermore, the charge state distribution of the outgoing beam implies that electron capture and loss processes are dominating mechanisms for the stopping of slow protons interacting with LiF.

To summarize, in our antiproton experiment on LiF we observe an \bar{p} stopping power around 50%–60% of that of protons. This reduction is of the same amount as for the metal-like materials investigated with antiprotons, which can be understood as a polarization effect [4,26]. The almost linear velocity dependence in the insulator LiF, however, remains unexplained.

This work has been supported by the Danish Natural Science Research Council (SNF). We also acknowledge the technical help of CERN staffs and the assistance and

advice from collaborators within the ASACUSA Collaboration. We thank Peter Sigmund for providing the data for stopping in LiF [21].

-
- [1] N. Bohr, *Philos. Mag.* **25**, 10 (1913).
 - [2] E. Fermi and E. Teller, *Phys. Rev.* **72**, 399 (1947).
 - [3] J. Lindhard, K. Dan. Vidensk. Selsk., *Mat. Fys. Medd.* **28**, No. 8 (1954).
 - [4] S. P. Møller, A. Csete, T. Ichioka, H. Knudsen, U. I. Uggerhøj and H. H. Andersen, *Phys. Rev. Lett.* **88**, 193201 (2002).
 - [5] W. H. Barkas, W. Birnbaum, and F. M. Smith, *Phys. Rev.* **101**, 778 (1956).
 - [6] S. P. Møller, E. Uggerhøj, H. Bluhme, H. Knudsen, U. Mikkelsen, K. Paludan, and E. Morenzoni, *Phys. Rev. A* **56**, 2930 (1997).
 - [7] R. Golser and D. Semrad, *Phys. Rev. Lett.* **66**, 1831 (1991).
 - [8] A. Schiefermüller, R. Golser, R. Stohl and D. Semrad, *Phys. Rev. A* **48**, 4467 (1993).
 - [9] D. Semrad, *Phys. Rev. A* **33**, 1646 (1986).
 - [10] M. Famá, J. C. Eckardt, G. H. Lantschner, and N. R. Arista, *Phys. Rev. Lett.* **85**, 4486 (2000).
 - [11] C. Auth, A. Mertens, H. Winter and A. Borisov, *Phys. Rev. Lett.* **81**, 4831 (1998).
 - [12] W. Schott, H. Daniel, F. J. Hartmann and W. Neumann, *Z. Phys. A* **346**, 81 (1993).
 - [13] H. Daniel, F. J. Hartmann, W. Neumann, and W. Schott, *Phys. Lett. A* **191**, 155 (1994).
 - [14] K. Eder *et al.*, *Phys. Rev. Lett.* **79**, 4112 (1997).
 - [15] M. Peñalba, J. I. Juaristi, E. Zarate, A. Arnau, and P. Bauer, *Phys. Rev. A* **64**, 012902 (2001).
 - [16] J. I. Juaristi *et al.*, *Phys. Rev. Lett.* **84**, 2124 (2000).
 - [17] P. Sigmund and A. Schinner, *Eur. Phys. J. D* **15**, 165 (2001).
 - [18] P. Sigmund and A. Schinner, *Nucl. Instrum. Methods Phys. Res., Sect. B* **195**, 64 (2002).
 - [19] P. Sigmund and A. Schinner, *Nucl. Instrum. Methods Phys. Res., Sect. B* **193**, 49 (2002).
 - [20] P. Sigmund, A. Fettouhi, and A. Schinner, *Nucl. Instrum. Methods Phys. Res., Sect. B* **209**, 19 (2003).
 - [21] A. Sharma, A. Fettouhi, A. Schinner, and P. Sigmund, *Nucl. Instrum. Methods Phys. Res., Sect. B* **218**, 19 (2004).
 - [22] I. Abril, R. Garcia-Molina, N. R. Arista and C. F. Sanz-Navarro, *Nucl. Instrum. Methods Phys. Res., Sect. B* **190**, 89 (2002).
 - [23] H. H. Andersen, A. Csete, T. Ichioka, H. Knudsen, S. P. Møller, and U. I. Uggerhøj, *Nucl. Instrum. Methods Phys. Res., Sect. B* **194**, 217 (2002).
 - [24] ICRU (International Commission on Radiation Units and Measurements, Inc.) Report No. 49, "Stopping Powers and Ranges for Protons and Alpha Particles," 1993.
 - [25] M. Bader, R. E. Pixley, F. S. Moser, and W. Whaling, *Phys. Rev.* **103**, 32 (1956).
 - [26] A. H. Sørensen, *Nucl. Instrum. Methods Phys. Res., Sect. B* **48**, 10 (1990).
 - [27] M. Kimura, *Phys. Rev. A* **47**, 2393 (1993).